International Journal of Engineering and Advanced Technology (IJEAT)
ISSN: 2249-8958 (Online), Volume-9 Issue-1S4, December 2019

Enhanced Productivity of Parabolic Solar Still Using α-Mno_2 Nano Particles

Selvakumar B., Arunachalam S., Vijaya Laxmi S.

Abstract: ***Parabolic solar still of area 0.25m² is designed using mild steel and its enhanced productive yield with □-MnO_2 nanoparticles had been analyzed. Microwave assisted solution method have been used to synthesis α-MnO_2 nanoparticles. XRD analysis of prepared □-MnO_2 nanoparticles size is found to be 35 nm. FTIR revealed the chemical composition and interaction of functional groups of MnO_2 nanoparticles. SEM image shows the aggregates are mostly particles with random shapes. HRTEM image confirms the average particle size was around 35 nm. From the optical study it is inferred that the energy band gap value as 2.69 eV and the conductivity of prepared nanoparticles is found to be in the order of 10^{-7} S cm^{-1}. Thermal stability of synthesized MnO_2 nanoparticle has been analyzed with the help of TG study. Electrical conductivity of MnO_2 have is in the order of 2.35×10^{-7} Scm^{-1} as calculated from AC impedance spectroscopy.***

Heat Transfer phenomena under internal and external transfer modes along with thermophysical properties such as thermal conductivity, dynamic viscosity, density and latent heat of distillate yield is calculated. Instantaneous efficiency of parabolic solar still without and with MnO_2 nanoparticles are found to be in the range of 11.52% to 40.71% and 10.94% to 46.32%. Similarly, overall efficiency is found to be 30.01% and 35.27%. The distillate productivity is mainly depended on the thermal parameters such as saturated vapor pressure and latent heat is observed as 8762 J/Kg, 9510 J/Kg, 2391875 Pa and 2388435 Pa for parabolic still in two modes of study.

Keywords: Distillate Yield, Heat Transfer, MnO_2, Parabolic Still, Temperature.

I. INTRODUCTION

MnO_2 nano particle shows a great potential as an alternative material among metal oxides because it is more economical, availability in abundance and is environment friendly. Manganese oxides long been known as materials of technological importance for catalytic and electro chemical applications. Various methods have been reported to synthesize such materials, including hydrothermal reaction [1], thermal decomposition [2], electro deposition [3, 4], template method [5] and micro emulsion method [6, 7]. There is several different crystallographic form of MnO_2, such as α, β, γ, δ, and ε- type. Due to the distinctive physico chemical properties along with various applications in fields such as catalysts [8], ion exchangers [9], magnetic materials [10], alkaline batteries [11] and super capacitors [12]. α-MnO_2 nanofibres mixed with aqueous and Dimethyl sulfoxide solvent by use of microwave reflux had been studied [13]. Of various available methods in synthesizing metal oxide nanoparticles, microwave assisted solution method have environmental approach along with several advantages such as rapid heating, energy saving, fine micro structure, better product quality, etc. Microwave assisted synthesis is cleaner, faster and economical than the conventional method. Microwaves are the electromagnetic radiations with wavelength ranging from 1mm to 1m in free space and frequencies between 300GHz to 300 MHz respectively. Microwave frequency used for carrying out the research is of 2.45 GHz, which is similar to the domestic microwave oven frequency. MnO_2 nanoparticle has been synthesized by microwave assisted method of solutions and its crystalline nature, chemical composition, morphology and optical studies were discussed in this work.

Fresh water requirement is the current trending problem faced in deserted and arid regions of the world where there are very less frequent rainfall. As a result of industrial and factory growth in rapid count, more and more is the depletion of fresh water resources. To satisfy the needs of the water for population in saline and brackish water area, solar desalination the only economical and eco-friendly way of producing the fresh water. Thrust research focus is carried out in areas of active and passive solar stills for the production of fresh water productivity [14, 15] along with design specifications. Enhancing the water productivity performance of the solar stills based on water depth, solar radiation, difference in water and air temperatures, thickness of top cover, basin area and wind velocity had been successfully carried out [16 to 19]. Results concluded that efficiency had been increased around 5-10% in carrying out optimum setup.

Influence of heat transfer coefficient in the enhanced distillate yield has been analyzed in detailed [15, 20, 21]. Result inferred that along with water temperature, evaporative, radiative and convective heat transfer from water to glass play a vital role in distillate yield. Role of phase change materials [22, 23, 24] in boosting the yield of solar stills concluded that the productivity increases around 10% to 15%. Ease of using acrylic material [25] for the top cover shows that because of low thermal conductivity of acrylic leads to the reduced loss of heat from top cover. Effect of nano particles (Al_2O_3 (or) CuO (or) Cu_2O) [26, 27, 28, 29] incorporated with basin material in enhancing the productive yield confirms that average of 10-20% increase in the efficiency of the system.

Manuscript published on 30 December 2019.
* Correspondence Author (s)
Selvakumar B.*, Department of Physics, School of Advanced Sciences, Kalasalingam Academy of Research and Education, Srivilliputtur, Tamil Nadu, India. selvakumar@klu.ac.in
Arunachalam S., Department of Chemistry, School of Advanced Sciences, Kalasalingam Academy of Research and Education, Srivilliputtur, Tamil Nadu, India. drarunachalam.s@gmail.com
Vijayalaxmi S., Department of Physics, Sri SRNM College, Sattur, Tamil Nadu, India. solarselva@gmail.com

In present study, combined performance of parabolic solar still without and with coated MnO_2 nano particle had been carried out and various parameters influencing the distillate yield had been calculated.

II. EXPERIMENTAL METHODOLOGY

A. Materials and Methods – MnO2 Nanoparticles

Two different anions of Manganese salts such as manganese II sulphate and manganese oxalate were used in the synthesis. Equal concentration of salts with 0.25 M is mixed each other at room temperature by continuous stirring. NaOH solution were added in drops while stirring till PH value of solution become 12. Solution is Stirred continuously at room temperature for 1 hour till it becomes pale brownish. Solution then transferred to house hold microwave oven to irradiate the mixer for 9 min. Later the product is cooled to room temperature. Collected by product is washed with deionized water and ethanol several time to remove impurities and it is dried under air atmosphere at a temperature of 70°C for 5 hours.

B. Design of Parabolic Solar Still

Hemispherical solar still of area 0.1661 m^2 (diameter of 0.56 m) is designed with the mild steel with dimension 0.56 m x 0.56 m x 0.15 m. For enhanced solar radiation absorption, water storage basin is coated with black mutty paint and filled with brackish water to a height of 0.05m. Water inlet provision is provided at a height of 0.12 m from the base. Similarly, the distillate yield collection provision with 0.02 m x 0.02 m dimension is placed on all the sides of the basin. ¼ inch outlet pipe is provided on four sides of water collection segment for distillate water collection.

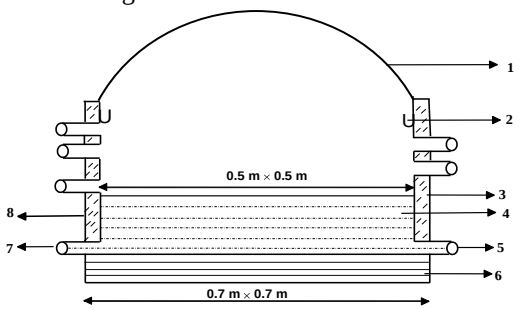

Fig. 1 Parabolic Solar Still - Cross sectional view

1. Still Top Cover
2. Distillate Collection Segment
3. Glass-wool Insulation
4. Water Storage Segment
5. Water Outlet
6. Base Insulation
7. Water Inlet
8. Outer Box

Fig. 2 Parabolic Solar Still - Photograph View

Transparent acrylic sheet of 3 mm thickness with transmittance 88% is used for parabolic top cover. Using cushion support and bolts, top parabolic cover is fixed to prevent air leakage or edge loss. Designed parabolic solar still is placed in a outer basin of dimension 0.70 m x 0.70 m x 0.25 m is made of plywood of 4mm thickness. Saw dust and glass wool is used as the insulation at base and sides.

III. EXPERIMENTAL ARRANGEMENT

Parabolic solar still had been designed using mild steel and is placed in terrace of solar energy laboratory. Performance analysis of the still had been carried out for black paint coated solar still and MnO_2 combined with back paint coated solar still on clear sunny days. 15 litre of saline water is filled in the water storage segment with pre-calibrated thermocouples at the appropriate places to measure the temperatures. Similarly, various temperatures such as air temperature inside still (T_{a1}), water temperature (T_{w1}), ambient temperature (T_{amb1}), top cover temperature (T_{g1}). Pyranometer is used to measure the total solar insolation (H). Distillate yield collected is measured by means of pre-calibrated measuring jar. Observations are carried out at regular time intervals of 30 min.

A. Heat Transfer in Parabolic Solar Still

For the operation of a conventional solar still, the most commonly used relationship to evaluate heat and mass transfer coefficients were proposed [30] and its applicability is verified over a wide range of operating temperatures within a solar still even at lower temperature ranges [31].

B. Internal Heat Transfer Modes

i) Convection

Due to the free convection of air, heat is transported inside the still which releases its enthalpy upon air coming into contact with the acrylic cover. Heat transfer per unit area per unit time due to convection is given by

$$Q_{ew1} = 0.884\left((T_{w1}-T_{g1})+\left(\frac{(P_w-P_g)(T_{w1}+273)}{268.9\,x10^3-P_w}\right)^{1/3}\right)(T_{w1}-T_{g1}) \quad (1)$$

ii) Evaporation

Dunkle connected convective heat transfer and obtained the expression for evaporative heat transfer coefficients as

$$Q_{ew1} = 16.273\ x10^{-3}\ h_{cw}\ R_1\ (T_{w1}-T_{g1}) \quad (2)$$

iii) Radiation

Radiative heat transfer coefficient is obtained using Stefan Bolzmann's constant and is given by,

$$Q_{rw1} = \sigma\ \varepsilon\left[(T_{w1}+273)^4-(T_{g1}+273)^4\right] \quad (3)$$

C. External Heat Transfer Modes

External convective heat transfer loss is due to the small thickness of the top cover. External convention loss from top cover to the outside atmosphere is,

$$Q_{ca1} = h_{ca1}(T_{g1}-T_{a1}) \quad (4)$$

here, h_{ca} is a function of wind velocity and is given [32] as,

$$h_{ca1} = 5.7 + 3.8\ V \quad (5)$$

External radiation loss from the acrylic cover to the atmosphere is given by,

$$Q_{ra1} = \varepsilon_g \sigma \left[(T_{g1} + 273)^4 - (T_{sky1} + 273)^4 \right] \quad (6)$$

Conduction heat loss through the base Q_{b1} is given by

$$Q_{b1} = h_{b1} (T_{w1} - T_{a1}) \quad (7)$$

IV. EFFICIENCY AND THERMAL PROPERTIES

Instantaneous distillate yield efficiency of the parabolic solar still is calculated using the formula

$$\eta = \left(\frac{M\ L}{H_s\ A\ t} \right) \quad (8)$$

By incorporating the condensation and evaporation temperatures, thermophysical properties [33] are estimated.

$$k = 0.0244 + (0.7673 \times 10^{-4})\ T_{av} \quad (9)$$

$$\mu = (1.718 \times 10^{-5}) + (4.620 \times 10^{-8})\ T_{av} \quad (10)$$

$$\rho = 353.44 / (273.35 + T_{av}) \quad (11)$$

$$h_v = 2324.6\ [(1.0727 \times 10^3) - (1.0167 T_{av}) + (1.4087 \times 10^{-4})\ T_{av}^2 - (5.1462 \times 10^{-6})\ T_{av}^3] \quad (12)$$

Temperatures of evaporation and condensation surface is expressed using the relation

$$T_{av} = (T_{w1} + T_{g1}) / 2 \quad (13)$$

Saturation vapour pressure and performance ratio of the solar still have been predicted using the expression [34]

$$P = 6893 \exp (54.63 - 12301/T' - 5.17 \ln T_1') \quad (14)$$

where $T_1' = (1.8T + 491.69)$

$$PR = (m_{e,i}\ h_v) / (H_s) \quad (15)$$

V. RESULTS AND DISCUSSION

XRD pattern of prepared α MnO_2 nanoparticle and α MnO_2 calcinated at 200ºC and 500ºC is shown in Fig. 3. It is found that all the peaks in fig correspond to (JCPDS data no 72-1982) tetragonal system having the significant peaks at 36.2º, 32.2º, 59.9º which can be indexed h k l values at (400) (100) (260). Good crystalline structure has been evidenced by strong diffraction peaks. Comparison concludes that when the prepared samples are calcinated, peak intensity has been increased but no change in the peaks positions. This shows the sample can't decompose before 500ºC. XRD pattern is obtained using X pert pro system with CuK α-radiation and the particle size is calculated using Scherer equation. The average particle size was around 35 nm.

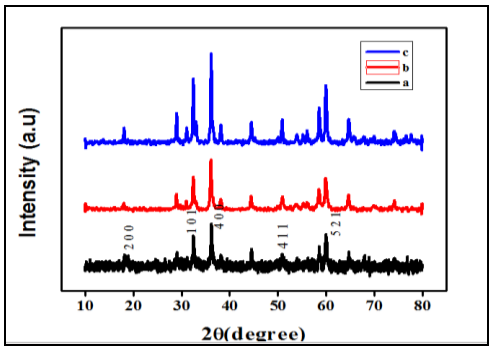

Fig. 3 XRD pattern for (a) MnO_2 (b) MnO_2 Calcinated at 200ºC (c) MnO_2 Calcinated at 500ºC

Fig. 4 shows a typical SEM image with panoramic view of the resulting product. It is inferred that the sample consists of aggregates of random shapes with size varying from hundreds of nanometer to few micrometer, which indicates that MnO_2 nanoparticles exhibit the agglomeration occurred during the synthesis due to the presence of Van der walls force.

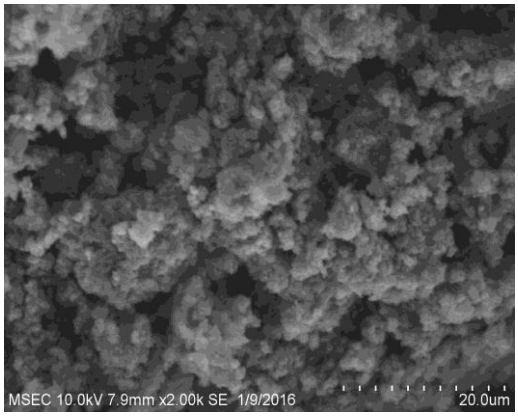

Fig. 4 SEM image of MnO_2 Nanoparticle

Fig. 5 shows high resolution TEM image of the prepared sample. Image shows that the product consists of particles with different sizes and shapes indicating the formation of aggregates. Average particle size of MnO_2 nanoparticle has been found around 35 nm. High magnifications of TEM image shows the clear lattice fringes were observed, which indicates the crystallinity of the sample. SEAD pattern shows the diffraction ring spot corresponds to phase selection with crystallinity.

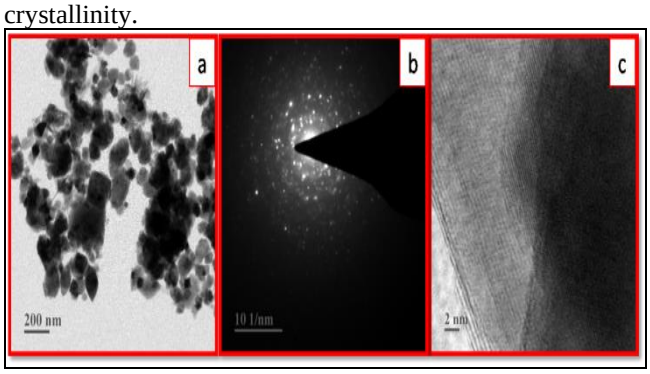

Fig. 5 HRTEM image of MnO_2 Nanoparticle.

Fig. 6 shows FTIR study of synthesized MnO_2 nano particle having two strong peaks 494 cm^{-1} and 604 cm^{-1} arising from the stretching vibration of Mn-O and Mn-O-Mn bonds indicating the formation of MnO_2 nanoparticle. Also, the absorption peak at 1112 cm^{-1} corresponds to the C-OH stretching and OH bending vibrations. Peaks at 1385 cm^{-1}, 1580 cm^{-1} and 1636 cm^{-1} correspond to C-OC hydroxyl stretching and O-H bending vibration. Results indicate the presence of few organic residues such as hydroxyl and carboxyl groups present on the surface of the MnO_2 nanoparticles. FTIR analysis graph matches the results in literatures [35, 36].

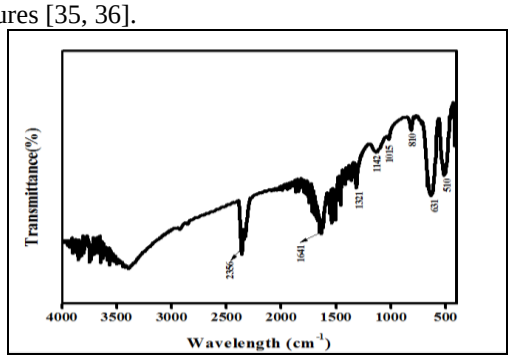

Fig. 6 FTIR study of MnO_2 Nanoparticle

Variation of water collection and solar radiation with time for parabolic still without and with MnO_2 nano particle is shown in Fig. 7. Amount of solar radiation received during the study is in the range of 422.7 W/m^2 to 1063 W/m^2 and 386.5 W/m^2 to 1063 W/m^2 for parabolic still performance study and parabolic still with MnO_2 nano particle.

Distillate water yield is in the range of 0.01 kg to 0.046 kg and 0.013 kg to 0.062 kg for the parabolic still study without and with MnO_2 nano particle. Since the top cover has the curved surface area, the impact of the ambient temperature over the still is more. Average difference in water and ambient temperature is found to be around 10 °C. Productivity yield is less during the warm up period than the later hours. Due to the decrease of water temperature and evaporation rate, distillate yield finally reduces at 8.00 p.m. Water collection of the parabolic still combined with MnO_2 nano particle is boosted due to the increase in absorptivity of more solar radiation by nano coated black paint.

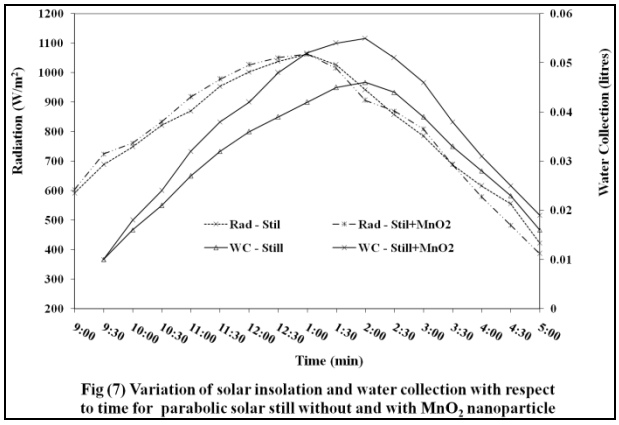

Fig (7) Variation of solar insolation and water collection with respect to time for parabolic solar still without and with MnO_2 nanoparticle

Instantaneous efficiency and performance ratio variation with time for parabolic solar still without and that combined with MnO_2 nanoparticle is shown in shown in Fig. 8. Efficiency variation is in the range of 11.52% to 40.71% and 10.94% to 46.32% for the still performance without and that combined with MnO_2 nanoparticle. Combined performance efficiency is higher than that of individual performance since black paint coated with MnO_2 nanoparticle absorbs more solar radiation. As a result, there is increase in productive yield.

Performance ratio observed to increase with time till steady state region is achieved and it starts to fall as the distillate yield drops. This is due to the reason that the rise in water temperature is being completely utilized for evaporation. Performance ratio obtained is in the range of 2.09% to 6.45 % and 2.01% to 7.60% for the parabolic still without and combined with MnO_2 nanoparticle.

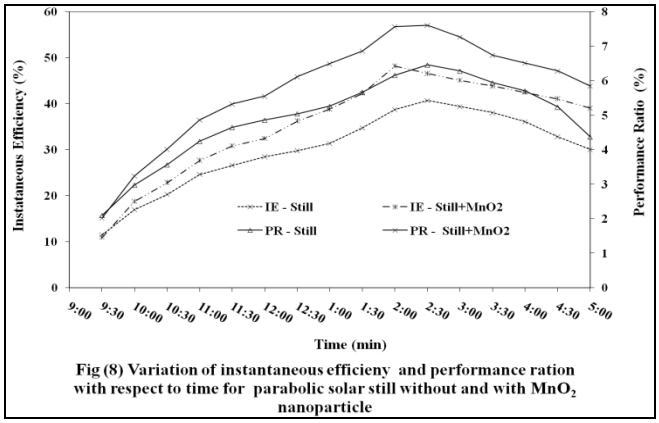

Fig (8) Variation of instantaneous efficieny and performance ration with respect to time for parabolic solar still without and with MnO_2 nanoparticle

Change in water temperature and thermal conductivity of water with respect to time for parabolic solar still and still combined with MnO_2 nanoparticle is shown in Fig. 9. Maximum value of water temperature is found to be 56.5 °C and 63 °C for parabolic solar still and still coated with MnO2 nanoparticle. Similarly, variation of room temperature is found to be in the range of 32 °C to 37.5 °C for both the study. Solar radiation is fully utilized in warming up the water temperature than the distillate yield during initial period. After attaining the maximum water temperature, it is fully utilized for evaporation of brackish water. Rise in water temperature results in the increase of saturated vapour pressure, which results in the increased productive yield of the solar still. More water collection is observed after warm up period which concludes that the maximum productivity yield is obtained only after reaching the optimum temperature.

Thermal conductivity of water is found to be 26.912x10^{-3} Wm^{-2} °C^{-1} to 28.236x10^{-3} Wm^{-2} °C^{-1} and 26.912x10^{-3} Wm^{-2} °C^{-1} to 28.447x10^{-3} Wm^{-2} °C^{-1} for parabolic still without and with MnO_2 nanoparticle. It is found that the thermal conductivity rises as the water temperature rises. Distillate yield of still coated with MnO_2 nanoparticles rises due to the higher values of thermal conductivity.

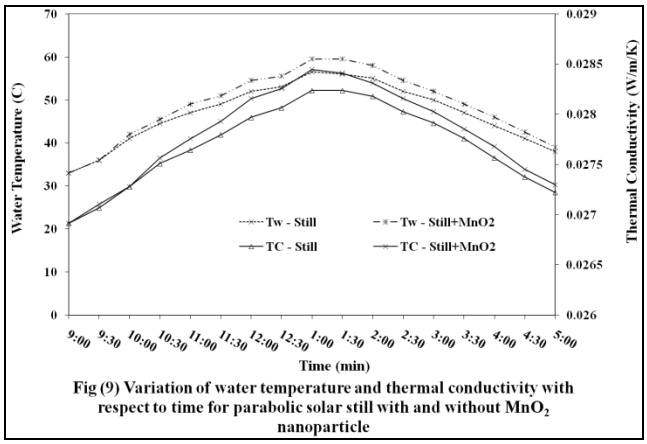

Fig (9) Variation of water temperature and thermal conductivity with respect to time for parabolic solar still with and without MnO_2 nanoparticle

Variation of saturation vapour pressure and latent heat with time factor is shown in Fig. 10. Saturation vapour pressure increase linearly as the radiation intensity rises, resulting in increase of distillate water collection. Saturation vapour pressure is observed to be 4911.15 to 12187.66 Pa for parabolic solar still and 4911.15to 13944.16 Pa for parabolic solar still coated with MnO_2 nanoparticle. Saturated vapour pressure have slight increase in values at higher temperature than that of warm up period.

It is fond that Latent heat starts to decreases during the warm up period and increases as water temperature drops. It infers that Latent heat value is minimum when water collection is maximum an vice versa. Latent heat value is found to be 2416127.4 to 2374750.69 kg^{-1} and 2416127.4 to 2368083.26 kg^{-1} for parabolic solar still without and with coated MnO_2 nano particle. Latent heat is used to boost the condensation during lower temperature. As a result of higher temperature in nano coated study, Latent heat values I found to be reduced than the normal study.

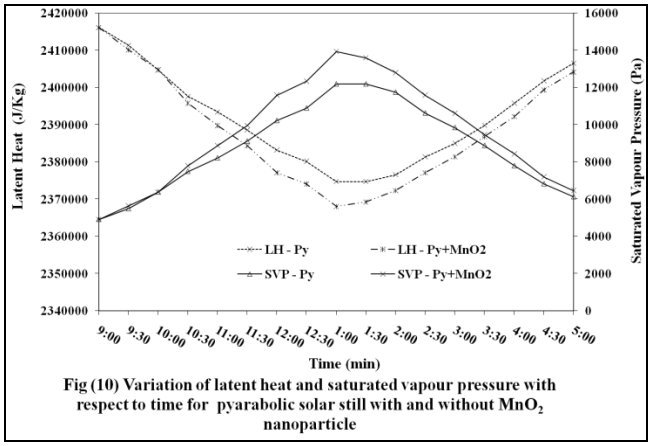

Fig (10) Variation of latent heat and saturated vapour pressure with respect to time for pyarabolic solar still with and without MnO_2 nanoparticle

Dynamic viscosity of water is found to be in the range of $18.69x10^{-6}$ Nsm^{-2} to $19.49x10^{-6}$ Nsm^{-2} and $18.692x10^{-6}$ Nsm^{-2} to $19.613x10^{-6}$ Nsm^{-2} respectively for parabolic still without and with coated MnO_2 nanoparticle. Thermal conductivity and dynamic viscosity if found to increase as the time progress and almost show the same trend.

Density of water is observed as $11.54x10^{-1}$ kgm^{-3} to $10.93x10^{-1}$ kgm^{-3} and $11.54x10^{-1}$ kgm^{-3} to $10.83x10^{-1}$ kgm^{-3} for both studies of parabolic solar still. This shows that as water temperature rises, there is a fall in the density of water.

Density of water is observed as $11.54x10^{-1}$ kgm^{-3} to $10.93x10^{-1}$ kgm^{-3} and $11.54x10^{-1}$ kgm^{-3} to $10.83x10^{-1}$ kgm^{-3} for both studies of parabolic solar still. This shows that as water temperature rises, there is a fall in the density of water.

TABLE I. HEAT TRANSFER VALUES

Study	Heat Transfer - Internal			Heat Transfer – External		
	Q_{ci} (W/m^2)	Q_{ri} (W/m^2)	Q_{ei} (W/m^2)	Q_{ce} (W/m^2)	Q_{re} (W/m^2)	Q_{be} (W/m^2)
Parabolic Still	14.238	48.469	127.14	38	86.893	4.941
Parabolic Still with MnO_2	16.425	54.694	156.81	44.985	91.561	5.608

VI. CONCLUSION

The present study indicates that parabolic solar still coated with α-MnO_2 nanoparticles has the capacity to produce more distillate yield because of high solar radiation absorbing capacity. Increase in the productivity yield is achieved due to higher values of thermal conductivity. Similarly, the electrical conductivity of MnO_2 is found to be in the order of 2.35×10^{-7} Scm^{-1} from AC impedance spectroscopy. The main advantage of this system is that the radiation received over the surface is equally entered in all sides of the still. Thus it raises the water temperature uniformly at all the place and also it has no shadow effect. Thus the water temperature of the still is increased to a more value compared to single slope and pyramid solar stills. Higher distilled water output yield makes parabolic solar still coated with α-MnO_2 will be a good option in the enhanced productivity and supply of fresh water.

ACKNOWLEDGMENT

Authors thank the management of Kalasalingam Academy of Research and Education, Anand Nagar, Srivillipttur for their constant encouragement and support and providing all facilities in carrying out the study.

REFERENCES

1. M. Xu, L. Kong, W. Zhou, and H. Li, "Hydrothermal Synthesis and Pseudocapacitance Properties of α-MnO2 Hollow Spheres and Hollow Urchins", *J. Phys. Chem. C*, vol. 111, issue. 51, pp. 19141-19147, 2007.
2. C. Yu, L. Zhang, J. Shi, J. Zhao, J. Gao and D. Yan, "A Simple Template-Free Strategy to Synthesize Nanoporous Manganese and Nickel Oxides with Narrow Pore Size Distribution, and Their Electrochemical Properties", *Advanced Functional Materials*, vol. 18, issue. 10, pp. 1544 – 1554, 2008.
3. Ran Liu and Sang Bok Lee, "MnO2/Poly(3,4-ethylenedioxythiophene) Coaxial Nanowires by One-Step Coelectrodeposition for Electrochemical Energy Storage", *J. Am. Chem. Soc*, vol. 130, issue. 10, pp. 2942-2943, 2008.
4. M. Nakayama, T. Kanaya, J.W. Lee, and B. N. Popov, "Electrochemical Synthesis of Birnessite-Type Layered Manganese Oxides for Rechargeable Lithium Batteries", *J. Power Sources*, vol. 179, issue. 1, pp. 361-366, 2008.
5. J.B. Fei, Y. Cui, X.H. Yan, W. Qi, Y. Yang, K.W. Wang, Q. He and J.B. Li, "Controlled Preparation of MnO2 Hierarchical Hollow Nanostructures and Their Application in Water Treatment", *Advanced Materials*, vol. 20, issue. 3, pp. 452-456, 2008
6. Hongmin Chen, Junhui He, Changbin Zhang and Hong He, "Self-Assembly of Novel Mesoporous Manganese Oxide Nanostructures and Their Application in Oxidative Decomposition of Formaldehyde", *J. Phys. Chem. C*, vol. 111, issue. 49, pp. 18033-18038, 2007.
7. Hongmin Chen and Junhui He, "Facile Synthesis of Monodisperse Manganese Oxide Nanostructures and Their Application in Water Treatment", *J. Phys. Chem. C*, vol. 112, issue. 45, pp. 17540-17545, 2008.
8. Steven L. Suib, "Structure, Porosity, and Redox in Porous Manganese Oxide Octahedral Layer and Molecular Sieve Materials", *J. Mater. Chem*., vol.18, pp. 1623-1631, 2008.
9. Steven L. Suib, "Porous Manganese Oxide Octahedral Molecular Sieves and Octahedral Layered Materials", *Acc. Chem. Res*, vol. 41, issue. 4, pp. 479-487, 2008.
10. X. Shen, A.M. Morey, J. Liu, Y. Ding, J. Cai, J. Durand, Q. Wang, W. Wen, W.A. Hines, J.C. Hanson, J. Bai, A.I. Frenkel, W. Reiff, M. Aindow and S.L. Suib, "Characterization of the Fe-Doped Mixed-Valent Tunnel Structure Manganese Oxide KOMS-2", *J. Phys. Chem. C*, vol. 115, issue. 44, pp. 21610-21619, 2011.
11. F. Y. Cheng, J. Chen, X. L. Gou and P. W. Shen, "High-Power Alkaline Zn–MnO2 Batteries Using γ-MnO2Nanowires / Nanotubes and Electrolytic Zinc Powder", *Advanced Materials*, vol. 17, issue. 22, pp. 2753-2756, 2005.
12. Y.L. Ding, C.Y. Wu, H.M. Yu, J. Xie, G.S. Cao, T.J. Zhu, X.B. Zhao and Y.W. Zeng, "Coaxial MnO/C Nanotubes as Anodes for Lithium-Ion Batteries", *Electrochimica Acta*, vol. 56, issue. 16, pp. 5844-5848, 2011.
13. E.K. Nyutu, C.H. Chen, S. Sithambaram, V.M.B. Crisostomo and S.L. Suib, "Systematic Control of Particle Size in Rapid Open-Vessel Microwave Synthesis of K-OMS-2 Nanofibers", *J. Phys. Chem. C*, vol. 112, issue. 17 pp. 6786-6793, 2008.
14. P. Vishwanath Kumar, Anil Kumar, Om Prakash, and Ajay Kumar Kaviti, "Solar Stills System Design: A Review", *Renewable and Sustainable Energy Reviews*, vol. 51, pp. 153-181, 2015.
15. S. Varun Raj and A. Muthu Manokar, "Design and Analysis of Solar Still", *Materials Today Proceeding*, vol. 4, issue. 8, pp. 9179-9185, 2017.
16. Ravishankar Sathyamurthy, Hyacinth J. Kennady, P.K. Nagarajan, and Amimul Ahsan, "Factors Affecting the Performance of Triangular Pyramid Solar Still", *Desalination*, vol. 344, pp. 383-390, 2014.
17. Karthikeyan Selvaraj, Alagumurthi Natarajan, "Factors Influencing the Performance and Productivity of Solar Stills - A Review", *Desalination*, vol. 435, pp. 181-187, 2018.
18. T. Arunkumar, Kaiwalya Raj, D. Dsilva Winfred Rufuss, David Denkenberger, Guo Tingting, Li Xuan and R. Velraj, "A Review of Efficient High Productivity Solar Stills", *Renewable and Sustainable Energy Reviews*, vol. 101, pp. 197-220, 2019.
19. D.G. Harris Samuel, P.K. Nagarajan, Ravishankar Sathyamurthy, S.A. El-Agouz and E. Kannan, "Improving the Yield of Fresh Water in Conventional Solar Still Using Low Cost Energy Storage Material", *Energy Conversion and Management*, vol. 112, pp. 125-134, 2016.

20. B. Selva Kumar, Sanjay Kumar and R. Jayaprakash, "Performance Analysis of a "V" Type Solar Still Using a Charcoal Absorber and a Boosting Mirror", *Desalination*, vol. 229, issues. 1–3, pp. 217-230, 2008.
21. M.R. Rajamanickam and A. Ragupathy, "Influence of Water Depth on Internal Heat and Mass Transfer in a Double Slope Solar Still", *Energy Procedia*, vol. 14, pp. 1701-1708, 2012.
22. Siddharaj V.Kumbhar, "Double Slope Solar Still Distillate Output Data Set for Conventional Still and Still With or Without Reflectors and PCM using High TDS Water Samples", *Data in Brief*, vol. 24, June 2019, 103852
23. Wen-Long Cheng, Yan-Kai Huo and Yong-Le Nian, "Performance of Solar Still Using Shape-Stabilized PCM: Experimental and Theoretical Investigation", *Desalination*, vol. 455, pp. 89-99, 2019.
24. Mousa Abu-Arabi, Mohammad Al-harahsheh, Hasan Mousa and Zobaidah Alzghoul, "Theoretical Investigation of Solar Desalination with Solar Still having Phase Change Material and Connected to a Solar Collector", *Desalination*, vol. 448, pp. 60-68, 2018.
25. A. Muthu Manokar and D. Prince Winston, "Comparative Study of Finned Acrylic Solar Still and Galvanised Iron Solar Still", *Materials Today: Proceedings*, vol. 4, issue. 8, pp. 8323-8327, 2017.
26. Peyman Zanganeh, Ataallah Soltani Goharrizi, Shahab Ayatollahi, Mehrzad Feilizadeh, "Productivity Enhancement of Solar Stills by Nano-Coating of Condensing Surface", *Desalination*, vol. 454, pp. 1-9, 2019.
27. S. Shanmugan, S. Palani and B. Janarthanan, "Productivity Enhancement of Solar Still by PCM and Nanoparticles Miscellaneous Basin Absorbing Materials", *Desalination*, vol. 433, pp. 186-198, 2018.
28. Bhupendra Gupta, Prem Shankar, Raghvendra Sharma and Prashant Baredar, "Performance Enhancement Using Nano Particles in Modified Passive Solar Still", *Procedia Technology*, vol. 25, pp. 1209-1216, 2016.
29. Saeed Nazari, Habibollah Safarzadeh and Mehdi Bahiraei, "Performance Improvement of a Single Slope Solar Still by Employing Thermoelectric Cooling Channel and Copper Oxide Nanofluid: An Experimental Study", *Journal of Cleaner Production*, vol. 208, pp. 1041-1052, 2019.
30. R.V. Dunkle, "Solar Water Distillation: Roof Type Still and a Multiple Effect Diffusion Still", International Development in Heat Transfer, A.S.M.E., Proc. International Heat Transfer, Part V, University of Colorado, pp. 895-901, 1961.
31. S. Adhikari, Ashvini kumar and G.D. Sootha, "Simulation Studies on a Multi-Stage Staked Solar Still", *Solar Energy*, vol. 54, issue. 5, pp. 317-323, 1995.
32. J.A. Duffie and W.A. Beckman, Solar Energy Thermal Process, John Wiley and Sons, New York, U.S.A, 1974.
33. S. Tayoma, T. Aragoki, K. Murase and T. Sumura, "Simulation of a Multi-Effect Solar Distillers", *Desalination*, vol. 45, pp. 101-110, 1983.
34. D.B. Brooker, F.W. Bakker-Arkma and C.W. Hall, Drying cereal grain, AVI West Port, U.S.A, 1978.
35. M. Zheng, Y. Liu, K. Jiang, Y. Xiao,and D. Yuan, "Alcohol-assisted Hydrothermal Carbonization to Fabricate Spheroidal Carbons with a Tunable Shape and Aspect Ratio", *Carbon*, vol. 48, issue. 4, pp. 1224-1233, 2010.
36. Marta Sevilla Dr, and Antonio B. Fuertes Dr, "Chemical and Structural Properties of Carbonaceous Products Obtained by Hydrothermal Carbonization of Saccharides", *Chem Eur J*, vol. 15, issue. 16, April 14, pp. 4195-4203, 2009.